Optimization of SINR and Illumination Uniformity in Multi-LED Multi-Datastream VLC Networks

Sifat Ibne Mushfique, Ahmad Alsharoa, *Member, IEEE*, and Murat Yuksel, *Senior Member, IEEE*

***Abstract*—Visible Light Communication (VLC), which is a recent technology that operates at the visible light spectrum band, is a very propitious technology complementary to RF in the era of spectrum crisis. Because of the extensive deployment of energy efficient Light Emitting Diodes (LEDs) and the advancements in LED technology with fast nanosecond switching times, VLC has gained a lot of interest recently. In this paper, we consider a downlink VLC architecture which is capable of providing simultaneous lighting and communication coverage across an indoor setting. We design a multi-element hemispherical bulb which transmits multiple data streams from its LEDs to mobile receivers. The architecture employs a Line-of-Sight (LOS) alignment protocol to tackle the hand-off issue caused by the mobility of the receivers in the room. We formulate an optimization problem that jointly addresses the LED-user associations as well as the LEDs' transmit powers in order to maximize the Signal-to-Interference plus Noise Ratio (SINR) while taking into consideration an acceptable illumination uniformity constraint across the room. We propose a near-optimal solution using Geometric Programming (GP) to solve the optimization problem, and compare the performance of this GP solution to low complexity heuristics.**

***Index Terms*—Visible Light Communication; illumination Uniformity; joint Optimization;**

I. Introduction

Visible Light Communications (VLC) is an emerging technology with significant potential to provide complementary wireless access speeds. As the number of Internet-of-Things (IoT) devices is exploding and the need for more aggregate wireless access capacity, VLC solutions are of high value. Recently, multi-element architectures in VLC systems have attracted attention by optical wireless communications researchers [1]–[3]. The multi-element VLC networks can offer increased aggregate throughput via simultaneous wireless links and attain higher spatial reuse. The downlink data transmission efficiency may be significantly improved by using multi-element VLC modules due to its light beam directionality where each transmitter, e.g., a Light Emitting Diode (LED), can be modulated with different data streams. Most of the VLC literature can be categorized into four groups based on the number of transmitters and datastreams involved in the design. Fig. 1 makes a visual comparison of these categories and Table I provides a high-level coverage of their design characteristics.

Single Element Single Datastream (SESD) designs are where one LED sends one datastream to one receiver. SESD VLC systems were heavily studied, especially in the early stages of VLC research, with a focus on modulation and data rate. In [4], the authors were able to show high speed data transmission using a phosphorescent white LED. 40 Mb/s speed was reported using On-Off Keying (OOK) modulation and more than 100Mb/s speed using Quadrature Amplitude Modulation (QAM), although the distance between the LED and photodiode was very small, i.e., 1cm. In a more practical setup demonstrated in [5], the authors were able to transmit data with a distance of 2.5m using off-the-shelf LEDs with 115Kb/s speed. In [6], performance of a novel LED lamp arrangement was investigated for reducing the Signal-to-Interference Noise Ratio (SINR) fluctuation from different locations in the room for multi-user VLC. They assumed that the illumination uniformity of the system would be maintained as the distribution of luminance had the same shape as that of the received optical power. This can be assumed only if the transmitters of the system have a fixed amount of source power in such a way that the received optical power in the room floor is uniform which is different from the case considered in this work. Another work [7] with emphasis on SINR proposed a coverage optimization model where genetic algorithm is used for optimizing LED arrangements. While maintaining the illumination requirement, a 75% improvement in communication coverage is attained. However, this work did not consider illumination uniformity though, and all the LEDs were assumed to have the same transmit power. In SESD designs, distance between the transmitter and the receiver plays a great role in data transmission speed.

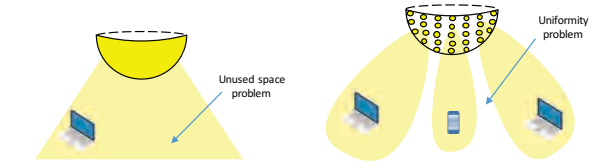

(a) Single-datastream: SESD or MESD

(b) Multi-datastream: SEMD or MEMD

Fig. 1: VLC architectures.

Single Element Multi Datastream (SEMD) designs have one LED sending multiple datastreams to multiple receivers. Significant amount of work explored how to use a single light source to serve multiple receivers, mostly via techniques involving diffuse optics and sharing of the VLC link. In [8], an outdoor VLC system is considered with a powerful light source to serve a large number of users accommodated by a big area. The work focused on the problem of using VLC system resources based on Time Division Multiple Access (TDMA) technique while aiming to maximize the spectral efficiency of the downlink fulfilling a Quality-of-Service (QoS) requirement. In [9], the authors analyzed a diffuse VLC Multiple-Input Multiple-Output

Sifat Ibne Mushfique and Murat Yuksel are with University of Central Florida (UCF), Orlando, Florida, USA. Email: sifat.im@knights.ucf.edu, murat.yuksel@ucf.edu.

Ahmad Alsharoa is with Missouri University of Science and Technology (MST), Rolla, Missouri, USA. Email: aalsharoa@mst.edu.

(MIMO) system taking Line-Of-Sight (LOS) propagation into account. Their simulation indicated that the angular diversity detectors had better performance over vertical oriented receivers for the mobile optical receivers.

Multi Element Single Datastream (MESD) techniques employ multiple LEDs that send one datastream to one receiver. In order to increase the received light intensity at the receiver, MESD designs use multiple LED sources sending the same data to a single receiver. Availability of multiple transmitters in MESD designs allows cooperative transmission [10], where the time of arrival from all the LEDs can be used to improve the detection probability of data bits at the receiver, and hence reduce BER. By employing multiple photo-detectors at the receiver, MESD designs also allow MIMO modulation techniques. Such MIMO VLC designs were shown to maximize data rate well with a modified singular value decomposition [11] while maintaining certain illumination requirements.

Multi Element Multi Datastream (MEMD) designs recently emerged and used multiple LEDs sending multiple datastreams to multiple receivers. Due to the additional flexibility in the multiplicity of elements and datastreams, more interesting MEMD VLC system combinations are possible based on LED placements and coverage of the illumination areas. The authors in [12] proposed a multi-cell VLC system for large area networks, where LED arrays in one cell can coordinate with LED arrays in the adjacent cells to cancel the inter-cell interference. In another recent work [13], Discrete Multi-Tone (DMT) modulation scheme has been shown to significantly improve the throughput of VLC in a room. In [14], the authors studied LED assignment problem in MEMD VLC systems taking proportional fairness and QoS requirement into consideration. They proposed suboptimal heuristic algorithms for LED assignment to receivers.

Illumination uniformity is an important factor to be considered in MEMD architecture where uniform light distribution needs to be considered as each LED's transmit power is being tuned. Otherwise, spotty lighting might emerge while the transmit powers of LEDs are being tuned for maximal SINR. Our work in this paper considers a more practical scenario than the previous works in the literature, where we jointly optimize the illumination uniformity with users' QoS. It is critical to ensure quality lighting in the room, while optimizing the LED assignment problem with a source power constraint on each LED. This type of MEMD architecture can improve the system performance as investigated in [15], [16].

TABLE I: Issues of different VLC architectures.

Issue	SESD	MESD	SEMD	MEMD
Simple architecture	✓	✓		
Complexity			✓	✓
Association problem			✓	✓
Special reuse			✓	✓
Handling multiple receivers				✓
Illumination problem			✓	✓
High data rate				✓

Thus far, we have covered many different aspect of studies in VLC and categorized them based on the number of transmitters and data streams in the design. The main differences of our work from the literature are presented below:

- While some of the previous works had illumination constraint by mainly focusing on improving the data rate, we are keeping illumination uniformity in our objective function, which can provide the best possible uniform lighting as well as the highest possible minimum SINR among all the users. So, we are optimizing both SINR and illumination uniformity at the same time.
- We consider the cases where LEDs have narrow divergence angles (e.g., less than 40^o) unlike the prior studies (including MIMO VLC [17]) that mainly looked at the scenarios using diffused light beams with large divergence angles.
- The biggest difference of our work is that we consider MEMD designs. The prior studies with multi-element designs in the literature only considered single datastream being sent to one of the users in the room [17]. In our case, we handle multiple datastreams, each of which is destined to a different user in the room. This brings the hard problem of LED-user association in addition to the SINR and uniformity maximization.

In this paper, we propose a novel MEMD framework by designing a multi-element bulb in a spherical shape consisting of multiple LEDs. This spherical shape allows high spatial reuse in addition to improving the illumination uniformity of the room. Each LED emits in a different direction, and hence, the spherical multi-element bulb can attain an evenly scattered lighting. Beyond the multi-element hemispherical bulb, to the best of authors' knowledge, this paper provides a framework for joint optimization of the LEDs' power and association to receivers to improve the aggregate data rate (of multiple data streams) and illumination uniformity in multi-element VLC networks for the first time. The main contributions are summarized as follows:

- Investigating a spherical multi-element bulb architecture in downlink VLC transmission, where each LED can be assigned to a receiver for data transmission or used for increasing the uniformity of illumination.
- Formulating an optimization problem that maximizes the ratio of SINR over the illumination uniformity taking into consideration the transmit peak power, minimum acceptable illumination uniformity, and LEDs-users associations.
- Solving the formulated optimization problem by finding the best LEDs' transmit power and the association between the LEDs and users. Therefore, the following two solution have been proposed:
  - Due to non-convexity of the problem, we firstly propose a benchmark solution by approximating the non-convex optimization problem into a convex optimization problem and solve it using Geometric Programming (GP) [18].
  - Then, we propose efficient low complexity partitioning algorithms to achieve near optimal practical solution.

The rest of the paper is organized as follows: Section II describes our spherical multi-element VLC architecture and

the system model of it. Our joint optimization problem is formulated and its NP hardness is proven in Section III. Near-optimal approximation solution to the problem is presented in Section IV, followed by heuristic approaches in Section V. Selected numerical simulation results are presented in Section VI. Finally, our work is summarized in Section VII.

II. MEMD VLC System Model

We consider a single hemispherical bulb for an indoor VLC system consisting of M LEDs serving U users. Each LED m transmits power equal to P_m Watt, $\forall m = 1, .., M$ as shown in Fig. 1(b). We also consider that the hemispherical bulb structure with two functions: Illumination of the room and wireless download to mobile users by acting as an access point for the room. It consists of multiple transmitters (i.e., LEDs) to facilitate simultaneous downloads to multiple receivers (i.e., users) as shown in Fig. 2. These LEDs are attached to the surface of the bulb in several layers pointing towards different directions so that they can illuminate different parts of the room. Furthermore, in addition to wireless communications, the LEDs are intended to provide light coverage in the room.

As the hemispherical bulb (which is the AP) has many transmitters attached to it, overall it has a broad coverage even in cases where each LED transmitter has a narrow beam. In fact, this is a key novelty of our work. We consider the cases where LEDs have narrow divergence angles which causes spotty lighting but attains pretty good throughput/SINR. Using smaller divergence angle for the transmitters decreases the chance of interference among multiple simultaneous data downloads as the overlapping of LED beams is less compared to the cases of larger divergence angles. To remedy the spotty lighting issue of our design, we make the illumination uniformity a key part of the optimization objective rather than just leaving it to a constraint which typically can be done as the light intensity being greater at a particular location on the room floor as in some of the earlier works [7].

We envision mobile users equipped with a Photo-Detector (PD) or a collection of PDs conformal to the surface of the unit with additional apparatus like lenses as appropriate. These users also need the capability of uploading using legacy Radio Frequency (RF) transmitters. Each receive a separate datastream download from the LED(s) with which they are in LOS alignment. The design of these units requires joint work of solid-state device and packaging as well as communication protocols. For instance, multi-element conformal PDs can be designed to cover a smartphone's or a laptop's surface, or multiple PDs can be used to attain a large field-of-view (FOV) [19] at the user.

Given multiple mobile users each downloading a different datastrem, our MEMD VLC system aims to attain high download speed for all users and smooth lighting across the room. To do so, the bulb structure will have to perform two tasks: (1) Partition LEDs to groups and assign each group to a user so that the user's download speed is maximized with minimal interference to the other downloads in the room, and (2) tuning transmit power of LEDS so as to maximize the illumination uniformity in the room. The ideal scenario would be to update the association and transmit power of the LEDs instantly, i.e. whenever there is a change in the position of any of the users, which is happening in our simulation as we are solving the optimization problem and calculating our objective function output based on several random sets of user coordinates. In a practical scenario, though, it would depend on the uplink speed of the RF transmitter of the user as the bulb will be able to start the process and update the association when it receives the acknowledgement from the receivers responding to the search frames periodically coming from the LEDs. Given the current system delays in the association process (e.g., the frequency of search packets being sent from the bulb, transmission delay of the search packets, the receivers processing delay upon receiving the search packets, the transmission delay of the acknowledgments from the receivers, and processing delay of the acknowledgments at the bulb), we are expecting the frequency of updating the association and transmit powers to be in the order of tens of milliseconds. Note that doing the update at several hundreds of milliseconds is also acceptable since human movement happens at larger timescales. More details of the association mechanism of our architecture can be found in one of our earlier works [1]. Next, we build a model of the system and formulate this joint optimization problem.

TABLE II: List of Key Symbols

Notation	Description
M	Number of LEDs
U	Number of users
N	Number of sensors in the room
B	Communication bandwidth
P_m	Transmit power of LED m
P	Maximum LED's transmit power
ϵ_{mu}	Association between LED m and user u
h_{mu}	Channel gain between LED m and user u
A_u	User PD area
d_{mu}	Distance between LED m and user u
φ_{mu}, ϕ_{mu}	Irradiance and incidence angles, respectively
ϕ_c	FOV angle of the PD
$Q_0(\varphi_{mu})$	Lambertian radiant intensity
q	The order of Lambertian emission
$\varphi_{1/2}$	The transmitter semiangle at half power
Γ_u	SINR at user u
ϑ	Illumination uniformity
α_0	The luminous efficiency
μ	Minimum acceptable illumination uniformity

A. Assumptions and Notation

For this study, we make the following assumptions:

- Each mobile user inside the room has one PD receiver and one RF transmitter, and is capable of extracting the desired signal from the optical transmitters.
- Locations of the mobile users are known to the access point, i.e., the bulb structure.
- There are N fixed light sensors assumed to be distributed uniformly inside the room. These sensors are not equipped with decoders and only used to ensure the illumination uniformity. Further, these sensors are not purposed for providing illumination, but rather for measuring illumination, and we do not need to employ them in a real scenario. We are solving this optimization problem for a multi-element VLC bulb whose dimensions are known

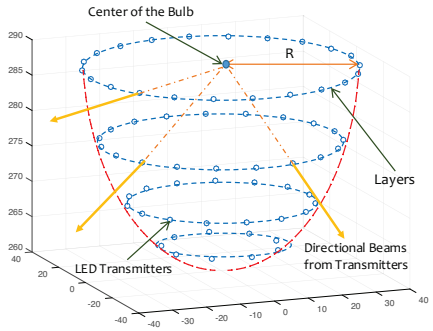

Fig. 2: Placement of transmitters in the multi-element bulb with 4 layers.

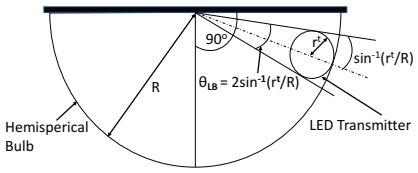

Fig. 3: Calculation of maximum number of layers in the bulb.

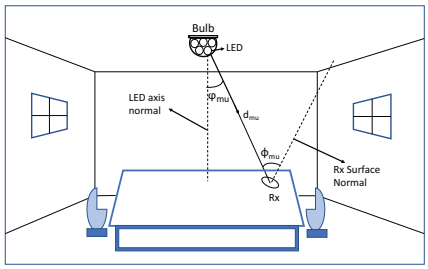

Fig. 4: Transmitters and Receivers in a VLC channel model.

and the room dimensions are fixed as well. These N sensors are used in our simulations in order to calculate the illumination level at the points on the floor, hence the illumination uniformity of the room. As far as the value of N is concerned, the larger it is, the more accurately we can calculate the illumination uniformity of the room. But after a certain point, it is not worthy to increase N for a larger runtime as we can reach a near perfect accuracy. From our experimentation, we found 100 sensors to be sufficient for the room size we consider.

To ease the rest of the discussion in the paper, we summarize our notation in Table II.

B. Layered Bulb Structure and Placement of LEDs

We place the LEDs on the hemispherical bulb on l layers as shown in Fig. 2. Let L be the maximum possible number of layers, and K_i is the maximum possible number of LED in the i-th layer. Depending on the shape of the bulb and LED transmitters[1], L and K can have different upper limits. To find the maximum number of layers L, we assume the LEDs to be spaced as closely as possible. First, we calculate how many LEDs can possibly be placed on the surface of any one half on the hemispherical bulb when looking from the x-z plane (y=0). So, each LED on the same layer will create the same angle with the center point of the bulb (since their radius is the same) which can be defined as:

$$\theta_{LB} = 2\sin^{-1}\left(\frac{r_t}{R}\right) \tag{1}$$

where r_t is the radius of an LED and R is the radius of the bulb. The factor 2 comes from the fact that we are using transmitter radius as our parameter for the calculation, and the angle the whole transmitter (with its diameter) creates with the center of the bulb is twice the angle it creates with its radius. Fig. 3 illustrates this more clearly. Then, the maximum number of layers for a particular r_t and R can be expressed as:

$$L = \left\lfloor \frac{90^o}{\theta_{LB}} \right\rfloor \tag{2}$$

[1]These LED transmitters may be composed of one or more LEDs. We assume that the transmitters are circular with a radius r_t=1.5cm, which can be implemented by multiple LEDs placed in a circle. We will keep referring to these circular transmitters as 'LEDs' or 'LED transmitters'.

where θ_{LB} is measured in degrees.

Next, we calculate the upper limit of the number of LEDs in a particular layer i. If the angle between the i-th layer and the perpendicular normal is θ_i, then the radius of circle created by the LED boards in the i-th layer will be:

$$r_{li} = R\cos\theta_i \tag{3}$$

Then, the angle created by each LED with the center of this circle will be:

$$\theta_{li} = 2\sin^{-1}(\frac{r_t}{r_{li}}) \tag{4}$$

Lastly, the maximum number of possible LEDs in the i-th layer can be calculated as:

$$K_i = \left\lfloor \frac{360^o}{\theta_{li}} \right\rfloor \tag{5}$$

where θ_{li} is measured in degrees. In our earlier work [2], we designed techniques to optimize the number of LEDs in each layer (i.e., k_i) up to these maximum values (i.e., K_i) for their corresponding layer. The key insight was to place more LEDs at the lower layers of the bulb as they contribute more for the achievable throughput. Thus, in this paper, we place the LEDs at the lower layers first and go up if more LEDs are available.

C. LED-User Association

Let us introduce a binary variable ϵ_{mu} that indicates the association between LED m and user u, and is given as follows:

$$\epsilon_{mu} = \begin{cases} 1, \text{if LED } m \text{ is associated with user } u. \\ 0, \text{otherwise.} \end{cases} \tag{6}$$

Following the MEMD model, we assume that user u can be associated to many LEDs at the same time. In contrary, any LED is not allowed to associate with more than one user simultaneously. Thus, the following constraint should be respected:

$$\sum_{u=1}^{U} \epsilon_{mu} \leq 1, \forall m. \tag{7}$$

D. Channel Model

In our channel model, we assume that the multipath propagation resulting from reflections and refractions is neglected and only LOS channel model is considered [20]. Therefore, the downlink communication channel between LED m and user u can be expressed as [21]

$$h_{mu} = \begin{cases} \frac{A_u}{d_{mu}^2} Q_0(\varphi_{mu}) \cos(\phi_{mu}) & , \ 0 \leq \phi_{mu} \leq \phi_c \\ 0 & , \ \phi_{mu} \geq \phi_c \end{cases} \tag{8}$$

where A_u is the user PD area and d_{mu} is the distance between LED m and user u. φ_{mu} and ϕ_{mu} are the irradiance and incidence angles, respectively (shown in Fig. 4). ϕ_c is the FOV angle of the PD. We have assumed that no optical filter is used. $Q_0(\varphi_{mu})$ is the Lambertian radiant intensity and expressed as

$$Q_0(\varphi_{mu}) = \frac{(q+1)}{2\pi} \cos^q(\varphi_{mu}), \tag{9}$$

where $q = -\ln(2)/\ln(\cos(\varphi_{1/2}))$ is the order of Lambertian emission and $\varphi_{1/2}$ is the transmitter semi-angle at half power.

Because of the nature of our system design (hemispherical bulb in the center of the room ceiling) the beams coming out from most of the LEDs in the bulb do not experience significant reflection. Beams coming from only a few number of LEDs in the higher layers of the bulb experience reflection from the side walls of the room. For this minimal effect of reflection, we do not consider it in our channel model to cut down the running time of our simulations.

E. SINR Calculation

We assume that each LED is either associated with one user or used for lighting only. Therefore, SINR at user u can be expressed as

$$\Gamma_u = \frac{{\beta_{uu}}^2}{N_0 B + \sum\limits_{\substack{k=1 \\ k \neq u}}^{U} {\beta_{ku}}^2} \tag{10}$$

where $\beta_{iu} = \sum\limits_{m=1}^{M} \epsilon_{mi} h_{mu} P_m$. β_{iu}, B and N_0 are the total power received by user i from its assigned LEDs, the communication bandwidth and the spectral density of the Additive White Gaussian Noise (AWGN), respectively.

F. Illumination Uniformity

Another important factor to be considered is illumination intensity distribution across the room floor. Specifically, the illumination uniformity, ϑ, can be defined as the ratio between the minimum and the average illumination intensity [22] among all N sensors, and is expressed as

$$\vartheta = \frac{\min\limits_{n}(\sigma_n)}{\frac{1}{N}\sum\limits_{n=1}^{N} \sigma_n} \tag{11}$$

where $\sigma_n = \sum\limits_{m=1}^{M} \alpha_0 P_m h_{mn}$ is the received total power at sensor n, α_0 is the luminous efficiency that depends on the LED color wavelength, h_{mn} is the channel between LED m and sensor n and $\min(.)$ is the minimum function. It should be noted that the illumination uniformity is based only on the illumination generated by the LEDs on the bulb which is P_m for a particular, LED m and the channels between M LEDs and N sensors which is h_{mn} for a particular m and n. It does not have any relation with the number of users U.

III. Problem Formulation

The approach of maximizing the total data rate which is known in the literature as Max C/I [23], promotes users with favorable channel and interference conditions by allocating to them most of the resources, whereas users suffering from higher propagation losses and/or interference levels will have very low data rates. Therefore, due to the unfairness of total sum data rate utility, the need for more fair utility metrics arises. For this reason, we choose to use Max-Min utility of the SINR. The Max-Min utilities are a family of utility functions attempting to maximize the minimum SINR in a network [24]. By increasing the priority of users having lower SINR, Max-Min utilities lead to more fairness in the network.

The key goal of our approach is to find solutions that balance illumination uniformity as well as communication efficiency, i.e., high SINR. As one of the key novelties in our work is considering the narrow beams from the LED transmitters which can cause uneven lighting in the room, we have placed illumination uniformity inside the objective function of our optimization problem. This ensures a more general approach to solve the problem of finding the best possible combination of illumination and communication. In this section, we formulate an optimization problem aiming to maximize the product of minimum SINR of all users ($\min\limits_{u}(\Gamma_u)$) and the illumination uniformity by taking into consideration the association and illumination intensity constraints. The optimization problem can be expressed as

$$\underset{\epsilon_{mu} \in \{0,1\}, P_m \geq 0}{\text{maximize}} \quad \min_{u}(\Gamma_u) \ \ \vartheta \tag{12}$$

subject to:

$$P_m \leq \bar{P}, \quad \forall m, \tag{13}$$

$$\sum_{u=1}^{U} \epsilon_{mu} \leq 1, \quad \forall m, \tag{14}$$

$$\vartheta \geq \mu, \tag{15}$$

where constraints (13) and (14) represent the power and association constraints, respectively. Constraint (15) is to ensure that the illumination uniformity is above a certain threshold, where μ is the minimum acceptable illumination uniformity for an indoor setting [22].

We consider the communication signal for LED m to be carried on the background DC light intensity with power P_m. And, for the case of only illumination, we assume that all LEDs are providing the same background light intensity with power P_m. This power can be adjusted to achieve the best possible SINR and lighting distribution in both the cases considered here. Basically, P_m is considered as the DC power when the LED is providing illumination only, and P_m is considered

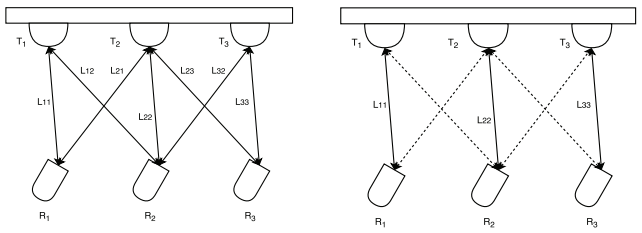

(a) Input graph of the problem with all possible links.

(b) Solution of the problem after removal of some links.

Fig. 5: Comparison with minimum ν-cut problem.

the average power when it is providing both illumination and communication. Similar assumptions can also be found at [14], [25].

In order to simplify the problem, we define new decision variables for minimum illumination $I_{\min}$ and minimum SINR $\Gamma_{\min}$, respectively, as

$$I_{\min} = \min_{n}(\sigma_n), \tag{16}$$

$$\Gamma_{\min} = \min_{u}(\Gamma_u). \tag{17}$$

Using these new variables, our optimization problem becomes

$$\underset{\substack{\epsilon_{mu}\in\{0,1\} \\ P_m, I_{\min}, \Gamma_{\min}\geq 0}}{\text{maximize}} \quad \frac{\Gamma_{\min} I_{\min}}{\frac{1}{N}\sum_{n=1}^{N}\sigma_n} \tag{18}$$

subject to:

$$\sigma_n \geq I_{\min}, \quad \forall n, \tag{19}$$

$$\frac{{\beta_{uu}}^2}{N_0 B + \sum_{\substack{k=1 \\ k\neq u}}^{U} {\beta_{ku}}^2} \geq \Gamma_{\min}, \quad \forall u. \tag{20}$$

and (13), (14), (15).

Notice that, the formulated optimization problem in (18)-(20) is a mixed-integer non-linear problem (MINP).

Algorithm 1 Decremental design for MIN_ν_CUT

```
procedure PARTITION(M,U)
while !solved do
  solved = MIN_ν_CUT(G(V,E))
  for i = 1 to M do
    for j = 1 to U do
      if if edge (i,j) ϵ solved then
        ϵ_ij = 1
      end if
    end for
  end for
end while
end procedure
```

A. NP-Completeness

We have found our optimization problem to be NP-complete by reducing it to the Minimum ν-cut problem, a well known NP-complete problem [26]. We define our main problem in (12) as $PARTITION\_WITH\_UNIFORMITY$ or $PARTITION\_WU$, and the minimum ν-cut problem as MIN_ν_CUT. Also, if we consider ϑ to be a fixed value between 0.7 and 1, then $PARTITION\_WU$ becomes a problem with fixed uniformity. We define this version of the problem as $PARTITION\_FOR\_FIXED\_UNIFORMITY$ or $PARTITION\_FFU$.

In MIN_ν_CUT, the input is a weighted undirected graph, $G(V, E)$ from which a set of edges needs to be removed such that the graph becomes a set of ν connected components with minimum weight [27]. The problem is NP-complete if we specify ν vertices and ask for the Minimum ν-cut which separates these vertices among each of the sets.

Now, if we consider every possible link between each transmitter and receiver in our MEMD VLC system (only considering the links where the receiver falls in the coverage area of the transmitter) then the collection of all these edges are similar to the input graph in the Minimum ν-cut problem. This is shown in Figure 5(a), where three transmitters on the bulb are named as T_1, T_2 and T_3, and three receivers are named as R_1, R_2 and R_3. The link between transmitter i and receiver j is named as L_{ij}. To make our problem comparable with MIN_ν_CUT, we first define a simplified version of the input graph $G(V, E)$ by assuming weight of these edges as the received signal strength from the LED to its assigned receiver, so the objective function described in (18) is dependent on these edges. Let this simplified version of the problem be $PARTITION$.

Lemma 1: *MIN_ν_CUT is polynominal time reducible to $PARTITION$, i.e., $PARTITION <_P MIN\_\nu\_CUT$.*
Proof: If we solve $PARTITION$ as if it is MIN_ν_CUT, then some edges from the input graph will removed so that the overall cost is the minimum. The ν vertices in MIN_ν_CUT is comparable with the number of receivers, and the ν connected components in the graph can be compared with the partitions in the bulb for the optimum assignment. Thus, this very simplified version of the problem, $PARTITION$, is NP-complete whereas the actual problem is even more difficult to solve as each link is dependent on the other links in most of the cases. This is due to the fact that, when calculating SINR for each receiver, signal coming from the transmitters other than the assigned one are treated as interference. Also, the illumination uniformity constraint (15) is another factor to consider in our original problem. Algorithm 1 shows that MIN_ν_CUT is convertible to $PARTITION$ in polynomial time.

Lemma 2: *$PARTITION$ is polynominal time reducible to $PARTITION\_FFU$, i.e., $PARTITION\_FFU <_P PARTITION$.*
Proof: We can reduce $PARTITION$ to $PARTITION\_FFU$ by considering μ as a set of t discrete values $\mu_1, \mu_2, ...\mu_t$ from 0.7 to 1, where t is a very large number. Thus, solving $PARTITION\_FFU$ iteratively for all these discrete uniformity values, we can find the solution of $PARTITION$. This is shown in Algorithm 2.

Theorem 1: *$PARTITION\_FFU$ is NP-Complete.*
Proof: It follows from Lemma 1 and Lemma 2.

Algorithm 2 Decremental design for $PARTITION$

procedure $PARTITION(M,U)$
$\mu \rightarrow \mu_1,\ \mu_2\ ...\ \mu_t$
while !$solved$ **do**
  for i = 1 to t **do**
    $solved = PARTITION\_FFU(m,u,\mu_i)$
  end for
end while
end procedure

Theorem 2: $PARTITION\_WU$ *is NP-Complete*.
Proof: By Theorem 1, $PARTITION\_FFU$ is proven to be NP-Complete. One can write an iterative algorithm similar to Algorithm 2 to show that $PARTITION\_WU$ is reducible to $PARTITION\_FFU$ in polynomial time. This proves $PARTITION\_WU$ is NP-Complete, too.

IV. Near Optimal Solution

In order to simplify the problem (12), we propose to approximate the joint optimization problem using Geometric Programming (GP). To do this, we first relax the variable ϵ_{mu} and make it continuous, i.e., $0 \leq \epsilon_{mu} \leq 1$. After obtaining an optimal value of ϵ_{mu}, we propose an efficient way to recover the best and closest upper integer value. We apply a successive convex approximation (SCA) approach to transform the non-convex problem into a sequence of relaxed convex subproblems that follows GP formulation [28].

A. Geometric Programming

GP deals with a class of nonlinear and non-convex optimization problems that can be solved after converting them to nonlinear but convex problems [29]. The standard form of GP is defined as the minimization of a posynomial function subject to inequality posynomial constraints and equality monomial constraints as given below

$$\underset{\boldsymbol{b}}{\text{minimize}} \qquad f_0(b) \tag{21}$$
subject to:
$$f_l(b) \leq 1, \quad \forall l = 1, \cdots, L, \tag{22}$$
$$\tilde{f}_{\tilde{l}}(b) = 1, \quad \forall \tilde{l} = 1, \cdots, \tilde{L}, \tag{23}$$

where $f_l(b)$, $l = 0, \cdots, L$ are posynomials and $\tilde{f}_{\tilde{l}}(z)$, $\tilde{l} = 1, \cdots, \tilde{L}$ are monomials. A monomial is defined as a function $f : \mathbf{R}^n_{++} \rightarrow \mathbf{R}$ as follows:

$$f(b) = \breve{a}\ b_1^{a_1} b_2^{a_2} ...\ b_Z^{a_Z}, \tag{24}$$

where the multiplicative constant $\breve{a} \geq 0$, and the exponential constants $a_z \in \mathbb{R}$, $z = 1, ..., Z$. A posynomial is a non-negative sum of monomials.

In general, GP in its standard form is a non-convex optimization problem, because posynomials and monomials functions are non-convex functions. However, with a logarithmic change of the variables, objective function, and constraint functions, the optimization problem can be turned into an equivalent convex form using the property that the logarithmic sum of exponential functions is convex (see [29] for more details). Therefore, the GP convex form can be formulated as

$$\underset{\boldsymbol{c}}{\text{minimize}} \qquad \log f_0(e^c) \tag{25}$$
subject to:
$$\log f_l(e^c) \leq 0, \quad \forall l = 1, \cdots, L, \tag{26}$$
$$\log \tilde{f}_{\tilde{l}}(e^c) = 0, \quad \forall \tilde{l} = 1, \cdots, \tilde{L}, \tag{27}$$

where the new variable $\boldsymbol{c}$ is a vector that consists of $[c_z] = [\log b_z]$. It can be noticed that (18)-(20) can be transformed to the GP standard form easily. In order to convert the optimization problem formulated in (18)-(20) to a GP standard form, we propose to apply approximation for constraint (19) and constraint (20). The single condensation method is employed to convert this constraint to posynomial as described below:

Definition 1: The single condensation method for GP involves upper bounds on the ratio of a posynomial over a posynomial. It is applied to approximate a denominator posynomial $g(b)$ to a monomial function, denoted by $\tilde{g}(b)$ and leaving the numerator as a posynomial, using the arithmetic-geometric mean inequality as a lower bound [28]. Given the value of b at the iteration $r-1$ of the SCA $b^{(r-1)}$, the posynomial g that, by definition, has the form $g(b) \triangleq \sum_{j=1}^{J} \mu_j(b)$, where $\mu_j(b)$ are monomials, can be approximated as:

$$g(b) \geq \tilde{g}(b) = \prod_{j=1}^{J} \left(\frac{\mu_j(b)}{\tilde{\mu}_j(b^{(r-1)})} \right)^{\tilde{\mu}_j(b^{(r-1)})}, \tag{28}$$

where $\tilde{\mu}_j(b^{(r-1)}) = \frac{\mu_j(b^{(r-1)})}{g(b^{(r-1)})}$. J corresponds to the total number of monomials in $g(b)$.

In order to convert constraints (19) and (20) to posynomials, we propose to apply the single condensation method given in Definition 1 to approximate the denominator posynomial to a monomial function, where in this case $J = M$ and $J = M(M+1)/2$ for constraints (19) and (20), respectively. Therefore, constraints (19) and (20) can be expressed respectively as

$$\frac{I_{\text{min}}}{\tilde{g}_1\left(P_m^{(r)}\right)} \leq 1, \forall n, \tag{29}$$

$$\frac{\Gamma_{\text{min}}\left(N_0 B + \sum\limits_{\substack{k=1 \\ k \neq u}}^{U} \beta_{ku}{}^2\right)}{\tilde{g}_2\left(P_m^{(r)}, \epsilon_{mu}^{(r)}\right)} \leq 1, \quad \forall u. \tag{30}$$

B. GP Standard Form Transformation

By considering the approximations of (29) and (30), we can formulate the GP approximated subproblem at iteration r of

the SCA as

$$\underset{\substack{\epsilon_{mu}^{(r)},P_m^{(r)},\\ \Gamma_{\min}^{(r)},I_{\min}^{(r)}\geq 0}}{\text{minimize}} \quad \frac{\frac{1}{N}\sum_{n=1}^{N}\sum_{m=1}^{M}\alpha_0 P_m^{(r)} h_{mn}}{\Gamma_{\min}^{(r)} I_{\min}^{(r)}} \tag{31}$$

subject to:

$$\frac{I_{\min}^{(r)}}{\tilde{g}_1\left(P_m^{(r)}\right)} \leq 1, \forall n, \tag{32}$$

$$\frac{\Gamma_{\min}\left(N_0 B + \sum_{\substack{k=1\\k\neq u}}^{U} {\beta_{ku}^{(r)}}^2\right)}{\tilde{g}_2\left(P_m^{(r)}, \epsilon_{mu}^{(r)}\right)} \leq 1 \quad \forall u, \tag{33}$$

$$\frac{P_m^{(r)}}{\bar{P}} \leq 1, \quad \forall m, \tag{34}$$

$$\sum_{u=1}^{U} \epsilon_{mu}^{(r)} \leq 1, \forall m, \tag{35}$$

$$\frac{\frac{\mu}{N}\sigma_n^{(r)} h_{mn}}{I_{min}} \leq 1 \tag{36}$$

The optimization problem given in (31)-(36) can be transformed to a convex form as given in (25)-(27). Therefore, each iteration of the SCA can be solved optimally as described in Algorithm 3 using any standard optimization methods [30]. Each GP in the iteration r loop (lines 3-5) tries to improve the accuracy of the approximations to a particular minimum in the original feasible region. This is performed until no improvement in the objective function is made. A parameter, $\xi \rightarrow 0$, is introduced to control the accuracy of the algorithm convergence of the objective function as follows: $|\chi^{(r)} - \chi^{(r-1)}| \leq \xi$.

Algorithm 3 SCA Algorithm

1: Select feasible initial values $\boldsymbol{b}^0 = [\epsilon_{mu}^{(0)}, P_m^{(0)}, \Gamma_{\min}^{(0)}, I_{\min}^{(0)}]$.
2: r=1
3: **while** Convergence ($|\chi^{(r)} - \chi^{(r-1)}| \leq \xi$) **do**
4: Approximate the denominators using the arithmetic geometric mean as indicated in (28) using $\boldsymbol{b}^{(r-1)}$.
5: Solve the optimization problem using the interior-point method to determine the new approximated solution $\boldsymbol{b}^{(r)} = [\epsilon_{mu}^{(r)}, P_m^{(r)}, \Gamma_{\min}^{(r)}, I_{\min}^{(r)}]$.
6: Update $r = r + 1$
7: **end while**

V. Heuristic Solutions

Since $PARTITION\_WU$ is an NP-Complete problem, we try to design heuristics with low complexity in terms of computation and memory. The users in the MEMD VLC system will be mobile and ad hoc. The existing users will move around in the room or leave the room, and new users will enter the room. These events will require the re-partitioning and re-assignment of LEDs to users and re-tuning of their transmit powers so as the keep the joint optimization objective high. Thus, it is crucial to minimize the time it takes to re-optimize the optimization parameters, which is the reason for us to design heuristics. We present two heuristics in this section and, later, compare them to the GP approximation by simulations.

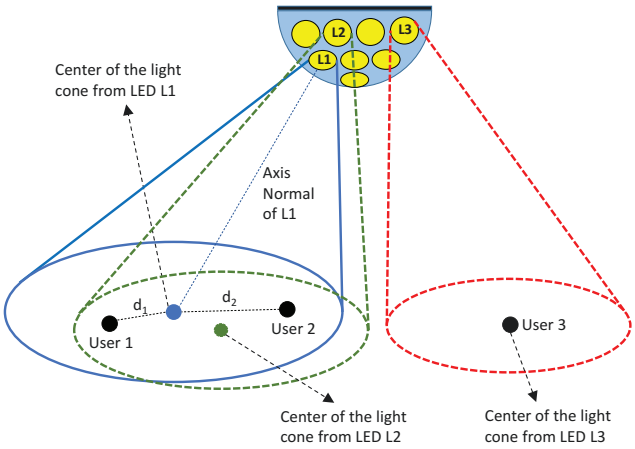

Fig. 6: A case of interference for an user: LEDs L1, L2 and L3 are assigned to user 1, 2 and 3 respectively. In this case, received power from L2 and L3 will be considered as interference at user 1 - since these LEDs are assigned to user 2 and user 3.

A. *SINR First Approach (SFA)*

In this approach, we propose to solve our optimization problem using a two-step iterative approach given the location coordinates of all users. In the first step, we optimize the LED-user association and the LED transmit powers that maximize the SINR. Then in the second step, by keeping the association fixed from the first step, we adjust only the LEDs' power level in order to achieve maximum objective function in (20) which is a function of SINR and illumination uniformity. The details of the proposed algorithm are as follows:

1) **Maximize SINR**
   a) We set a maximum power value, P_{max}, that can be assigned to an LED. We use P_{max} = 100 mW.
   b) We assign LED m to the closest user to its beam projection if the user lies in the cone of LED m.
   c) If there is no user in the cone, then also P_{max} is allocated to LED m initially and it is not assigned to any of the users.
   d) If there is more than one user in the cone of LED m, then we assign this LED to the user which is nearest to the center of the cone of the LED, but with fractional power, since there will be interference in this case. For simplicity, we calculate this fraction by taking the distances of the nearest and second nearest user from the center of the LED cone into account. For example, if the distance of the nearest user from the center of the cone is d_1 and the distance of the second nearest user from the center of the cone is d_2 then the allocated power to LED m would be, P_m = P_{max}(1-d_1/d_2) (shown in Fig. 6). When the second nearest user is much closer to the nearest user, the ratio of d_1 and d_2 is higher, and that makes the value of P_m to be lower to minimize the effect of interference.

After assigning all M LEDs in this fashion (which focuses on SINR) we try to improve the illumination uniformity in the next step.

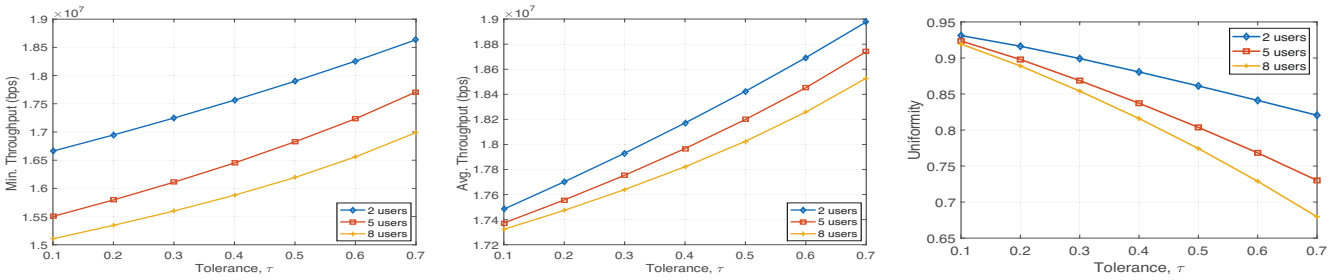

(a) Minimum throughput vs. tolerance for 2, 5 and 8 users. $M = 391$. and $\theta_d = 40^o$.

(b) Average throughput vs. tolerance for 2, 5 and 8 users. $M = 391$. and $\theta_d = 40^o$.

(c) Illumination uniformity vs. tolerance for 2, 5 and 8 users. $M = 391$ and $\theta_d = 40^o$.

Fig. 7: Effect of τ on throughput and uniformity for UFA.

2) **Maximize Uniformity**
   a) We set four discrete power levels (i.e., P_{max}, $P_{max}/2$, $P_{max}/3$, $P_{max}/4$) which can be allocated to the LEDs that are unassigned instead of allocating them the full power. We allocate these discrete power levels to the LEDs which are unassigned and equipped with full power.
   b) We then recalculate the illumination uniformity using (11) and select the discrete power values for the LEDs that gives the maximum uniformity.

This heuristic gives a lower priority to the illumination uniformity and aims to maximize SINR with low complexity while trying to achieve an acceptable illumination uniformity.

B. Uniformity First Approach (UFA)

In SFA, we try to maximize the SINR by assigning as much power as possible to the LEDs which have only one user in their cones, then try to improve the illumination uniformity. In the UFA, we do the opposite - we try to find the allocated power values of the LEDs for the best possible illumination uniformity, then we modify these power values to improve the SINR. The approach is described below:

1) We formulate a quasi-convex optimization problem that can be solved efficiently using bisection [29] to obtain the allocated power values for the LEDs for maximum possible uniformity, where the optimal solution is obtained for a fixed SINR value, i.e., $\Gamma_{\min}$ is constant. This problem can be formulated as

$$\underset{P_m, I_{\min} \geq 0}{\text{minimize}} \quad \frac{\frac{1}{N}\sum_{n=1}^{N} \sigma_n}{\Gamma_{\min} I_{\min}} \qquad (37)$$
subject to (13), (19).

   We denote the resulting P_m values as intermediate power values which are P_{1i}, P_{2i}, ... P_{Mi} for M LEDs.
2) When there is only one or no user in LED m's cone, then we proceed like Step 1(c) in SFA but with a little difference. Instead of allocating maximum power to LED m, we allocate $\max(P_{mi}(1+\tau), P_{max})$. We try different values for τ, from 0.1 to 0.7 which is a measurement of how much we can deviate the allocated power to LED m from its intermediate value P_{mi}.
3) Then, we proceed like Step 1(d) in SFA but with a little difference. The equation for the allocated power to LED m will be P_m = P_{mi}(1-d_1/d_2). We also make sure that P_m is within the tolerance limit we set, thus $P_m \geq P_{mi}(1-\tau)$.

This approach gives more priority to the illumination uniformity and makes sure that the minimum uniformity constraint in (15) is satisfied as τ gets closer to 0. A larger tolerance limit τ allows UFA to deviate from the uniformity-satisfying transmit power values for a higher throughput. In essence, τ can be used as a knob to tune UFA between optimizing for uniformity and throughput. Tuning τ enables flexibility in our approach to solve the joint optimization problem. The designer of the VLC system could tune τ in our formulation in order to attain solutions favoring higher throughput or more uniform illumination while still satisfying the minimum illumination constraint followed by the previous studies in the literature. This effect of τ can be seen in Fig. 7, where we plot minimum throughput, average throughput and illumination uniformity vs. the tolerance value τ for 2, 5 and 8 users cases. As described earlier, minimum and average throughput gradually increase while uniformity gradually decreases for higher value of τ.

A critical design issue to consider in our problem is the dynamic nature of the VLC system in terms of the number of users, since it can change at any time with arrival or departure of users. In order to find solutions attaining higher SINR than what our approach finds, it may be possible to solve a traditional VLC SINR maximization problem [7] by feeding an appropriate minimum illumination constraint to the optimizer, e.g., approximately 0.925 for an attained minimum throughput of 15.2 Mbps from Fig. 7). However, this minimum illumination threshold changes depending on the user count and positions in the system. Thus, it would be necessary to find the appropriate illumination threshold before using the SINR maximization approach. Our approach allows a more flexible framework. The tolerance variable τ enables us to run a fast heuristic to find a good solution when the number of served users or positions change. Further, using our approach, the designer of the VLC system can get the highest possible illumination uniformity with zero tolerance, and then improvement of the minimum throughput (SINR) is possible in two ways:

First, the designer can increase τ up to 1 while making sure the threshold of minimum allowable illumination uniformity is

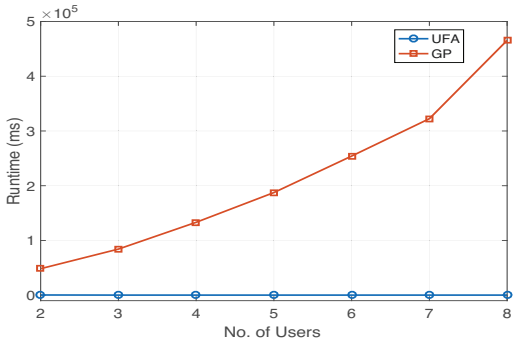

Fig. 8: Runtime vs. No. of users for UFA and GP. $M = 65$.

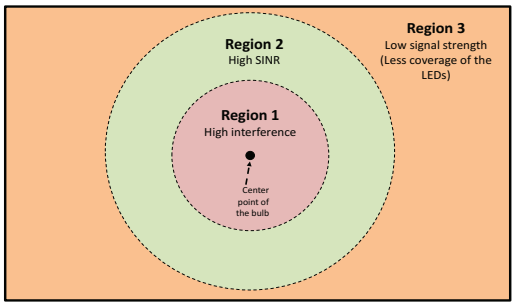

Fig. 9: Difference in signal strength across the room floor assuming the hemispherical bulb in the center of the ceiling.

maintained (which is the constraint (15) in our formulation) in search of a higher SINR.

Second, with $\tau > 0$, the designer can quickly find a good solution to learn the minimum illumination uniformity for that solution and then solve a traditional VLC SINR maximization problem [7] with the learned illumination uniformity threshold to search for a higher SINR.

Although in the second approach we may be able to find a higher SINR, we will need to run the optimizer for each of these τ values and for each time the total number of users is changed - which is highly time-consuming. This is where the approach presented in our paper is most useful as we will need to run the optimizer only once - which can be to find the maximum illumination uniformity for a particular bulb configuration, and then from that we can find SINR for different τ values, and user count and positions. Thus, this approach takes less time overall while it is yet capable of obtaining a near optimal SINR if required.

C. Computational and Memory Complexity

We are assuming M total LEDs and N total sensors in our problem. In both UFA and SFA, we check each of the LEDs to allocate source power and assign it to a user if needed. This effectively takes $O(M)$ time. The majority of the time is needed in calculating h_{mu} and h_{mn}, which take $O(MU)$ and $O(MN)$, respectively. h_{mn} is only calculated once since user coordinates do not affect the communication channel between the LEDs and sensors. So, we can ignore the $O(MN)$ complexity from the h_{mn} calculation as it will only be done when the VLC system is initialized. Thus, the overall running time complexity of both SFA and UFA is $O(MU)$.

Regarding the memory complexity, in both approaches we have to store the coordinates of M LEDs to calculate h_{mu} and h_{mn}. We store the value of h_{mu} and h_{mn} too, which takes space of $O(MU)$ and $O(NU)$ respectively. SINR and illumination uniformity variables takes space of $O(U)$ and $O(N)$, respectively. So, overall the memory complexity of SFA and UFA is $O((M+N)U)$.

Calculating the complexity of the GP solution is not very straightforward as we use the 'fmincon' command of MATLAB in order to get the solution of our constrained nonlinear multi-variable objective function. In order to compare the GP solution with UFA in terms of running time, we the runtime versus number of users plot to observe the growth with respect to the growing number of users, which is shown in Fig. 8. We can clearly see that even for a small number of user range (2 to 8) the running time for GP starts to grow very quickly whereas for UFA it remains almost the same. This is the most important advantage of UFA over GP.

TABLE III: Simulation Parameters

Parameter	Value
Room Size	6m x 6m x 3m
Radius of the hemispherical bulb, R	40cm
Number of LEDs on the bulb, M	391
Radius of an LED transmitter, r_t	1.5cm
Divergence angle of the LEDs, θ_d	40^o, 50^o
Maximum transmit power of the LEDs, P	0.1W
Radius of a PD receiver*, r_r	3.75cm
Number of users, U	2-8
Number of sensors, N	100
Visibility, V	0.5km
Optical signal wavelength, λ	650nm
AWGN spectral density, N_0	2.5 x 10^{-20} W/Hz
Modulation bandwidth, B	20MHz
Minimum uniformity, μ	0.7

*We assume that an array of PDs is used to attain a large receiver area.

VI. Simulation Results

In this section, we provide simulation results to study the performance of our MEMD VLC system model. Our aim is to see if the SFA and UFA heuristics can attain performance close enough to the GP solution, and identify any notable outcomes emerging from our designs. We focus on two metrics: *Minimum throughput* among the users and illumination *uniformity*. To compare our proposed methods (SFA, UFA, and GP), we use exact same input parameters for all of them. We randomly placed the users on the room floor with their receiver's FOV normal looking towards the ceiling. We report the average of the minimum throughout and illumination uniformity results among these randomly generated cases. To gain confidence in our results, we repeated the simulation experiments 300 times for all the results.

We use white LEDs with luminous efficiency $\alpha_0 = 60$ lumen/watt [31]. The default values of the remaining input parameters used in our simulations are given in Table III. For placing LEDs on the bulb, we followed the method in Section II-B. In particular, for a bulb with R = 40cm radius, we place M = 391 LEDs on 20 layers with $k_{1..20}$ = [1, 6, 12, 15, 19, 26, 30, 37, 43, 33, 30, 28, 25, 21, 16, 13, 11, 10,

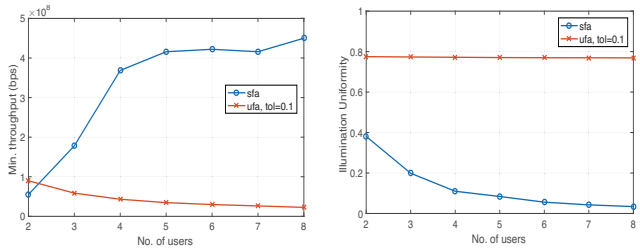

(a) Minimum throughput vs. No. of users. $\theta_d = 50^o$.

(b) Illumination uniformity vs. No. of users. $\theta_d = 50^o$.

Fig. 10: Comparison between UFA and SFA.

9, 6]. The throughput and uniformity results we will present are likely to be attained by fewer LEDs; however, we want to observe the potential performance our heuristic and use a high number of LEDs in the simulation experiments.

A. UFA versus SFA

First, we compare the two heuristic approaches, UFA and SFA to see whether one performs significantly better. We have compared both minimum throughput among the users and illumination uniformity for 2 to 8 users for these two approaches, as seen in Fig. 10(a) and Fig. 10(b). As we can see, minimum throughput and uniformity decrease for both approaches with increased number of users. Also, as expected, UFA gives better uniformity and SFA gives better minimum throughput. Although SFA gives a higher minimum throughput compared to UFA, the uniformity is poor and practically unacceptable, as typically the illumination uniformity of an indoor setting should be at least close to μ=0.7. UFA is able to maintain this uniformity target even for 8 users. So, from this point on, we choose UFA to be the preferred heuristic solution as it is able to maintain an acceptable uniformity value although it has produced lower minimum throughput.

B. GP Solution versus UFA

In order to understand how close our heuristics can get to our near-optimal solution via GP, we compare it to our preferred heuristic solution, UFA, with different tolerance values. An impediment is the time complexity of the GP solution. Since it takes too long to run GP, we reduce the LED count M on the bulb to make it tractable with our computation capabilities. Following the method in Section II-B, we place M = 65 LEDs on 7 layers with $k_{1..7}$ = [1, 11, 14, 17, 10, 7, 5].

In Fig. 11(a) and 11(b), we observe that GP solution obtains much better minimum throughput compared to UFA but the uniformity is a little lower in some cases where $\tau = 0.25$, as it tries to put more balance in the objective function output towards throughput. It is clear from Fig. 11(c) that, for the objective function, the GP beats UFA for all tolerance values. Although GP has a higher objective function output in all the cases, UFA can come close in terms of minimum throughput for higher τ values and in terms of uniformity for lower τ values. This is verifying our intuitions that τ can be used to tune UFA's balance between throughput and uniformity.

C. Effect of Number of Users on UFA

Although UFA yields lower objective function output values in comparison to GP, a huge advantage of it is a much lower complexity. With GP, it becomes even more time-consuming to calculate the minimum throughput or uniformity in case of a high number of users (8 and above) whereas it can be done relatively quickly using UFA. Thus, we analyze how the throughput and uniformity changes when more users are added to the system. As shown in Fig. 12, the minimum throughput continues to decrease for higher number of users as expected, and a good uniformity value is maintained by UFA even for a very high number of users. Although marginal reduction in the minimum throughput is large early on (e.g., going from 2 to 3 users causes about a 3-fold decrease in minimum throughput), it is notable that UFA maintains a high minimum throughput even when the room is crowded. For instance, even though the number of users in the room increases by a 10-fold, the reduction in minimum throughput is also by 10-fold (from $\approx 10^8$Bits/s to $\approx 10^7$Bits/s). Further, we observe that higher tolerance does not yield much improvement on the minimum throughput as seen in Fig. 12(a).

D. UFA with Different Room Sizes

We also look at how minimum throughput and uniformity is affected by different room sizes and shapes, e.g., the room gets more rectangular. To observe this, we keep increasing the width of the room by 1m at a time and keep the length of the room constant. Results are seen in Fig. 13. As the room floor gets more rectangular, spaces are more at both sides, so the chances of the users being more scattered increases, which means there are less chances of interference. But, with higher number of users, interference is going to be more likely, thus the throughput decreases. In the case of uniformity, it becomes increasingly difficult to maintain balanced lighting with the width of the floor being significantly greater than the length, which explains the dip in uniformity for more rectangular room floors (Fig. 13(b)). Although, in case of small number of users, we can see the opposite scenario in Fig. 13(a). Whenever we are making the room more rectangular, it decreases the possibility of interference as they are going to be more scattered, but at the same time it increases the possibility of a user being in a 'low signal strength' region where there is much less transmitter coverage (these regions are shown in Fig. 9). After a particular number of users in the system the second possibility becomes more dominant over the first one, which explains the transitions in Fig. 13(a).

E. Effect of Divergence Angles with UFA

We also look at the effect of divergence angle of the LEDs with UFA. We use 3 divergence angle values = 10^o, 20^o and 40^o. In Fig. 14(a), 14(b), and 14(c), we observe minimum throughput, average throughput and uniformity, respectively. As we can see, throughput for 10^o and 20^o is higher because of less interference since the beams are too directional, but this hampers the uniformity a lot as well. The average throughput for 10^o goes higher than 20^o for more than 4 users, as we see

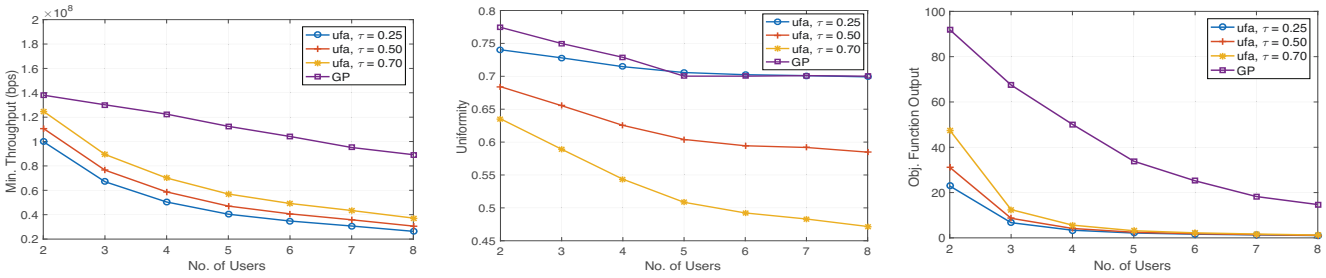

(a) Minimum throughput vs. No. of users. (b) Illumination uniformity vs. No. of users. (c) Objective function value vs. No. of users.

Fig. 11: Comparison between GP and UFA with $M = 65$ and $\theta_d = 50^o$.

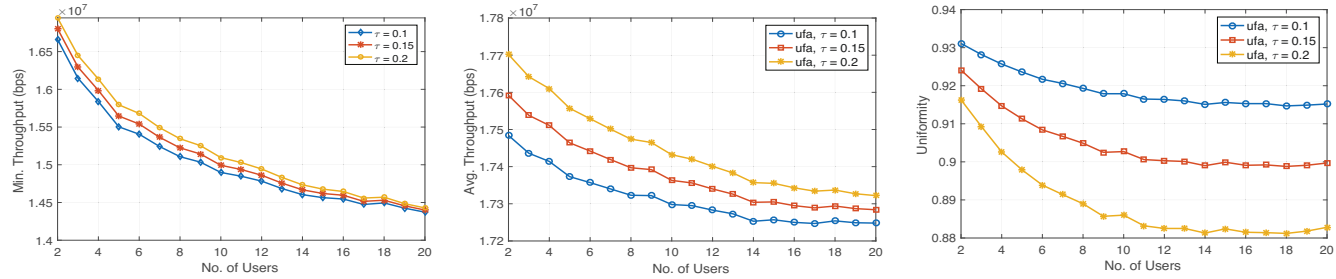

(a) Minimum throughput vs. No. of users,upto 20. (b) Average throughput vs. No. of users,upto 20. (c) Illumination uniformity vs. No. of users, upto 20.

Fig. 12: Throughput and Uniformity for many users for UFA. $M = 391$ and $\theta_d = 40^o$.

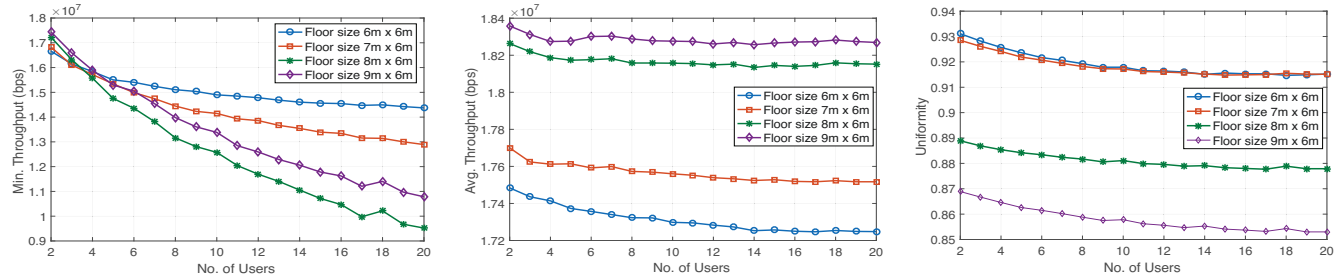

(a) Minimum throughput vs. No. of users,upto 20. (b) Average throughput vs. No. of users,upto 20. (c) Illumination uniformity vs. No. of users upto 20.

Fig. 13: Throughput and Uniformity for different room sizes. $M = 391$ and $\theta_d = 40^o$.

in Fig. 14(b). When the number of users are less than or equal to 4, the possibility of high interference with higher divergence angle is dominant enough to keep the throughput higher, but after that, the effect of interference becomes too high, making the throughput better for lesser divergence angle. Performance in the case of 40^o is the best among these cases since a very balanced lighting is obtained with the ability to cover more users, as a result not hampering the average throughput too much.

F. Effect of Bulb Radius on UFA

We try to see the effect of different bulb radius on the system for UFA. As shown in Fig. 15, we plot minimum and average throughput as well as uniformity versus the number of users for $R = 40cm, 50cm, 60cm$ and $70cm$. We can see that the decline of minimum throughput is the least in the case of 40 cm bulb radius, the value we have typically used. Uniformity is almost the same for all cases though a little better for higher bulb radius, as the LED beams can cover a little more space in the corner of the room floor. Average throughput is a little higher for greater bulb radius as the more expanded beam distribution is the cause of relatively less interference. We can see a small transition like Fig. 13(a) in Fig. 15(a), as the possibility of a particular user being in a 'less coverage' area is low for a small number of users, so higher bulb radius gives just a little better throughput in this case. But the mentioned possibility is significant enough in the case of more than 3 users, which makes the minimum throughput value lower for the higher bulb radius.

G. Heatmaps of the Transmit Power of LEDs with UFA and GP

To explore how the transmit powers of the LEDs are allocated with our proposed algorithms, we plot the projection point from

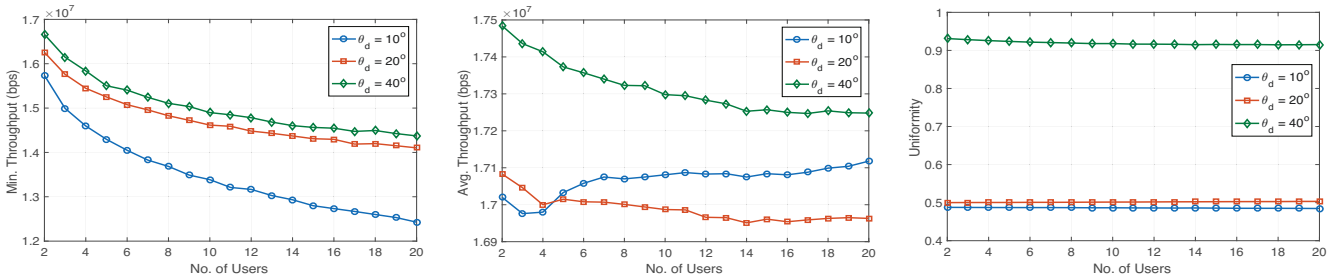

(a) Minimum throughput vs. No. of users for different divergence angles. (b) Average throughput vs. No. of users for different divergence angles. (c) Illumination uniformity vs. No. of users for different divergence angles.

Fig. 14: Comparison between different divergence angles in UFA. $M = 391$.

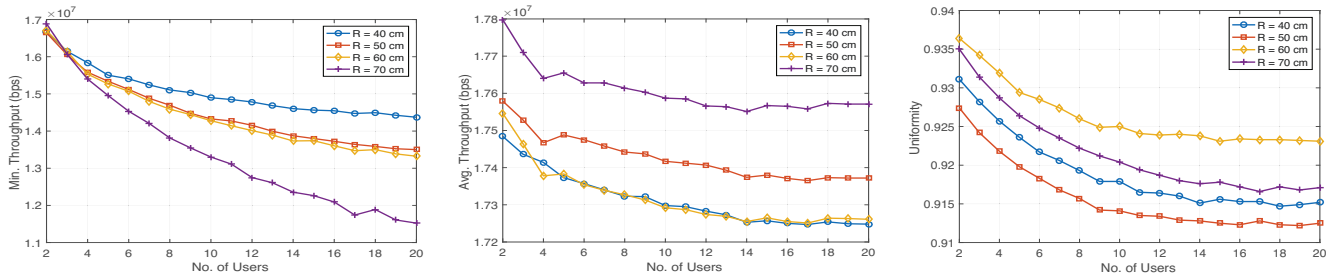

(a) Minimum throughput vs. No. of users for different bulb radius. (b) Average throughput vs. No. of users for different bulb radius. (c) Illumination uniformity vs. No. of users for different bulb radius.

Fig. 15: Comparison between different bulb radius in UFA. $M = 391$ and $\theta_d = 40^o$.

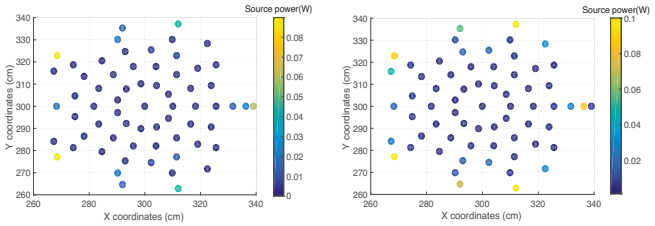

(a) Heatmaps of the transmit power of LEDs with UFA. $M = 65$. (b) Heatmaps of the transmit power of LEDs with GP. $M = 65$.

Fig. 16: Heatmaps of the transmit power of LEDs with UFA and GP.

the top of each LED on the floor using different colors, where the color of a particular projection point of an LED indicates the amount of transmit power of that LED. Like subsection VI-B, The higher the LEDs are in the bulb, the more outwards their projections points are in floor. As we can see in Fig. 16, transmit power of the LEDs in the higher layers are more than those of the lower layers in the bulb. This is to maintain a good uniformity as the LEDs in the higher layers cover the corner (darker) spots in the room.

VII. Summary and Future Work

In this paper, we explored in a multi-element multi-datastream (MEMD) VLC architecture where VLC is used for downlink and RF for uplink. For the downlink, we have formulated the problem of resolving tuning LED transmit powers and LED-user association as an optimization problem. The optimization problem takes the users' throughput and illumination uniformity into consideration and handles dynamic assignment of the transmitters to react to the mobility of users. We showed the problem is NP-Complete.

For the MEMD VLC downlink and access optimization, we proposed a near-optimal approximation solution and two suboptimal heuristic solutions, i.e., SINR First Approach (SFA) and Uniformity First Approach (UFA). We have analyzed the performance of the two heuristic solutions and found that UFA is significantly better. We, then, compared UFA with the near-optimal solution and found out that it is not far away from the near-optimal approach. A key insight is that one can design low complexity heuristics for the MEMD VLC downlink problem. From our simulations, for reasonable assumptions about the LEDs and bulb size, we observed that UFA can attain about 10Mbps minimum throughput while keeping illumination uniformity higher than 0.7 for up to 20 receivers in a 36m^2 room.

Several future works are possible related to the MEMD VLC downlink approach. For the partitioning problem, other heuristic algorithms may be explored to attain results that are closer to the optimal solution. It would be interesting to see the how the proposed algorithms perform with different system parameters (e.g., room shape, shape of the bulb) and whether there are any relationship between them. In our work, we considered receivers/users up to 20. Designing MEMD VLC downlink and access techniques that can work for thousands of receivers in the room is also a worthy direction.

References

[1] S. I. Mushfique, P. Palathingal, Y. S. Eroglu, M. Yuksel, I. Guvenc, and N. Pala, "A software-defined multi-element vlc architecture," *IEEE*

Communications Magazine, vol. 56, no. 2, pp. 196–203, 2018.
[2] S. I. Mushfique and M. Yuksel, "Optimal multi-element vlc bulb design with power and lighting quality constraints," in *Proc. of the 3rd ACM Workshop on Visible Light Communication Systems (VLCS), New York, USA*, 2016, pp. 7–12.
[3] M. S. Mossaad, S. Hranilovic, and L. Lampe, "Visible light communications using OFDM and multiple LEDs," *IEEE Transactions on Communications*, vol. 63, no. 11, pp. 4304–4313, Nov. 2015.
[4] J. Grubor, S. C. J. Lee, K. Langer, T. Koonen, and J. W. Walewski, "Wireless high-speed data transmission with phosphorescent white-light LEDs, berlin, germany," in *Proc. of the 33rd European Conference and Exhibition of Optical Communication*, Sep. 2007, pp. 1–2.
[5] Y. Yang, X. Chen, L. Zhu, B. Liu, and H. Chen, "Design of indoor wireless communication system using LEDs," in *Proc. of the Communications and Photonics Conference and Exhibition, Shanghai, China*, Nov. 2009, pp. 1–2.
[6] Z. Wang, C. Yu, W.-D. Zhong, J. Chen, and W. Chen, "Performance of a novel led lamp arrangement to reduce snr fluctuation for multi-user visible light communication systems," *Optics express*, vol. 20, no. 4, pp. 4564–4573, 2012.
[7] J.-H. Liu, Q. Li, and X.-Y. Zhang, "Cellular coverage optimization for indoor visible light communication and illumination networks," *Journal of Communications*, vol. 9, no. 11, pp. 891–898, 2014.
[8] A. M. Abdelhady, O. Amin, A. Chaaban, and M.-S. Alouini, "Resource allocation for outdoor visible light communications with energy harvesting capabilities," in *Proc. of the IEEE Global Communications Conference Workshops (GLOBECOM Workshop), Singapore, Singapore*, Dec. 2017, pp. 1–6.
[9] P. F. Mmbaga, J. Thompson, and H. Haas, "Performance analysis of indoor diffuse VLC MIMO channels using angular diversity detectors," *IEEE Journal of Lightwave Technology*, vol. 34, no. 4, pp. 1254–1266, Feb. 2016.
[10] G. B. Prince and T. D. C. Little, "On the performance gains of cooperative transmission concepts in intensity modulated direct detection visible light communication networks, valencia, spain," in *Proc. of the 6th IEEE International Conference on Wireless and Mobile Communications*, Sept. 2010, pp. 297–302.
[11] P. M. Butala, H. Elgala, and T. D. Little, "SVD-VLC: A novel capacity maximizing VLC MIMO system architecture under illumination constraints," in *Proc. of the IEEE Global Communication Conference Workshops (GLOBECOM Wkshps), Atlanta, GA, USA*, Dec. 2013, pp. 1087–1092.
[12] T. V. Pham, H. Le Minh, and A. T. Pham, "Multi-cell VLC: Multi-user downlink capacity with coordinated precoding," in *Proc. of the IEEE International Conference on Communications Workshops (ICC Workshops), Paris, France*, MAy 2017, pp. 469–474.
[13] D. Bykhovsky and S. Arnon, "Multiple access resource allocation in visible light communication systems," *IEEE Journal of Lightwave Technology*, vol. 32, no. 8, pp. 1594–1600, Apr. 2014.
[14] Y. S. Eroğlu, İ. Güvenç, A. Şahin, Y. Yapıcı, N. Pala, and M. Yüksel, "Multi-element VLC networks: LED assignment, power control, and optimum combining," *IEEE Journal on Selected Areas in Communications*, vol. 36, no. 1, pp. 121–135, Jan. 2018.
[15] Z. Chen, D. Tsonev, and H. Haas, "Improving SINR in indoor cellular VLC networks," in *Proc. of the IEEE International Conference on Communications (ICC), Sydney, Australia*, June 2014, pp. 3383–3388.
[16] A. Tsiatmas, F. M. J. Willems, and S. Baggen, "Optimum diversity combining techniques for VLC systems," in *Proc. of the IEEE Global Commnication Conference Workshops (GLOBECOM Workshop), Austin, TX, USA*, Dec. 2014, pp. 456–461.
[17] K.-H. Park and M.-S. Alouini, "Improved angle diversity non-imaging receiver with a help of mirror in indoor mimo-vlc systems," in *IEEE Wireless Communications and Networking Conference (WCNC)*. IEEE, 2018, pp. 1–6.
[18] M. Chiang, C. W. Tan, D. P. Palomar, D. O'neill, and D. Julian, "Power control by geometric programming," *IEEE Transactions on Wireless Communications*, vol. 6, no. 7, pp. 2640–2651, July 2007.
[19] T. Q. Wang, Y. A. Sekercioglu, and J. Armstrong, "Analysis of an optical wireless receiver using a hemispherical lens with application in mimo visible light communications," *J. Lightwave Technol.*, vol. 31, no. 11, pp. 1744–1754, Jun 2013.
[20] I. Moreno and C.-C. Sun, "Modeling the radiation pattern of LEDs," *Optics Express Journal*, vol. 16, no. 3, pp. 1808–1819, Feb. 2008.
[21] H. Marshoud, P. C. Sofotasios, S. Muhaidat, G. K. Karagiannidis, and B. S. Sharif, "On the performance of visible light communication systems with non-orthogonal multiple access," *IEEE Transactions on Wireless Communications*, vol. 16, no. 10, pp. 6350–6364, Oct. 2017.
[22] I. Standardization, "Lighting for work places part 1: Indoor (ISO: 8995-1: 2002 e)," *International Commission on illumination, Vienna*, 2002.
[23] X. Bi, J. Zhang, Y. Wang, and P. Viswanath, "Fairness improvement of maximum c/i scheduler by dumb antennas in slow fading channel," in *IEEE 72nd Vehicular Technology Conference-Fall*, 09 2010, pp. 1–4.
[24] Y. Song and G. Li, "Cross-layer optimization for OFDM wireless networks-Part I: Theoretical framework," *IEEE Transactions on Wireless Communications*, vol. 4, no. 2, pp. 614–624, Apr. 2005.
[25] H. Wu, Q. Wang, J. Xiong, and M. Zuniga, "SmartVLC: When smart lighting meets VLC," in *Proceedings of the 13th International Conference on emerging Networking EXperiments and Technologies*. ACM, 2017, pp. 212–223.
[26] O. Goldschmidt and D. S. Hochbaum, "Polynomial algorithm for the k-cut problem," in *Proc. of the 29th IEEE Annual Symposium on Foundations of Computer Science*, 1988, pp. 444–451.
[27] Wikipedia. (2017) Minimum k-cut Wikipedia, the free encyclopedia. [Online; accessed Dec.,2017]. [Online]. Available: https://en.wikipedia.org/wiki/Minimum k-cut
[28] A. Alsharoa, H. Ghazzai, A. E. Kamal, and A. Kadri, "Optimization of a power splitting protocol for two-way multiple energy harvesting relay system," *IEEE Transactions on Green Communications and Networking*, vol. 1, no. 4, pp. 444–457, Dec. 2017.
[29] S. Boyd and L. Vandenberghe, *Convex Optimization*. New York, NY, USA: Cambridge University Press, 2004.
[30] M. Grant and S. Boyd, "CVX: Matlab software for disciplined convex programming, version 2.1," http://cvxr.com/cvx, Mar. 2014.
[31] B. music Netherlands. (2017) Lite gear LED PAR 30 7w lamp WW Edison 45gn. [Online]. Available: https://www.bax-shop.nl/producten-uit-assortiment/lite-gear-led-par-30-7w-lamp-ww-edison-45g

Sifat Ibne Mushfique has completed his B.Sc. in Electrical & Electronic Engineering from Bangladesh University of Engineering and Technology (BUET) in 2011 and is currently a Ph.D. candidate in the department of Computer Engineering at the University of Central Florida (UCF), Orlando, FL. His research interests include the area of Optical Wireless Communications, and majorly Visible Light Communication. He likes playing table tennis and participating in competitive programming in his free time.

Ahmad Alsharoa (SM'14-M'18-SM'19) was born in Irbid, Jordan. He received the PhD degree with co-majors in Electrical Engineering and Computer Engineering from Iowa State University (ISU), Ames, Iowa, USA, in May 2017. He is currently an assistant professor at Missouri University of Science and Technology. His current research interests include: wireless networks, UAV and HAP communications, edge computing, optical communications, internet of things (IoT), energy harvesting, and self-healing networks.

Murat Yuksel (SM'11) is an Associate Professor at the ECE Department of the University of Central Florida (UCF), Orlando, FL. He received his M.S. and Ph.D. degrees in computer science from RPI in 1999 and 2002, respectively. His research interests are in the area of networked, wireless, and computer systems with a recent focus on big-data networking, UAV networks, optical wireless, public safety communications, device-to-device protocols, economics of cyber-security and cyber-sharing, routing economics, network management, and network architectures. He has been on the editorial board of Computer Networks, and published more than 150 papers at peer-reviewed journals and conferences and is a co-recipient of the IEEE LANMAN 2008 Best Paper Award.